Integration of stream geomorphic assessment data with low-complexity hydraulic models to improve floodplain mapping

30 September 2021

Technical Report

Vermont Water Resources and Lake Studies Center

Prepared by:

Kristen L. Underwood, PhD, Department of Civil & Environmental Engineering, UVM
Rebecca M. Diehl, PhD, Department of Geography, UVM
Jeremy E. Matt, Department of Civil & Environmental Engineering, UVM
Stephanie Drago, Department of Civil & Environmental Engineering, UVM

Table of Contents

Suggested citation:

Underwood, K.L., Diehl, R.M., Matt, J.E., Drago, S. (2021). Integration of stream geomorphic assessment data with low-complexity hydraulic models to improve floodplain mapping. Technical report to the Vermont Water Resources and Lake Studies Center.

Abstract

Low-complexity hydraulic modeling approaches (e.g., HAND) are increasingly applied to map floodplain inundation extents across large regions. These approaches require minimal parameterization and rely on readily-available topographic data sets, that have improved in resolution in recent years. Still, these modeling approaches have limitations in representing channel-floodplain coupling due to their reliance upon average river geometry calculated over hydrologically-defined (NHD) reaches that may span sub-reaches of variable valley confinement or slope. Thus, new modeling approaches are needed that incorporate reach-scale geomorphic data for channels and (dis)connectivity status of floodplains to better predict flooding extents and depths, and quantify the uncertainty of these estimates.

We present results of a pilot study in two Vermont watersheds to transfer a probabilistic modeling approach (probHAND) from NHD reaches to reaches defined from stream geomorphic assessments (SGAs). To examine integrity of this approach, we compared the probHAND-modeled floodplains to a floodplain generated using a hydrodynamic model (1D HEC-RAS) in the Mad River watershed. We then compared floodplains generated from NHD reaches to those generated from SGA reaches, and evaluated geomorphic metrics that may account for variability between the two approaches, in both the Mad River and Black Creek watersheds.

Overall, floodplains built on SGA reaches and NHD reaches had a similar performance when compared to a 1D HEC-RAS floodplain for the 1% annual exceedance probability event along the Mad River main stem. However, at a reach scale, we found that the SGA floodplain captured more variability in inundation patterns where the HAND approach is sensitive to errors in geomorphic parameters, such as in low gradient, unconfined settings where small changes in predicted depth have significant impacts on inundation area. We also found that the SGA floodplain captured more variability in inundation patterns than the NHD floodplain for the 100-year floodplain in hydraulically complex reaches, coinciding with the village centers of Moretown, Waitsfield and Irasville.

Floodplain mapping built on geomorphically-defined reaches is likely to improve accuracy of flood stage predictions, notably close to town centers and along low-gradient settings, to better quantify flood hazards posed to riverside infrastructure. Improved fidelity of modeled inundation extents will help to better characterize the nutrient retention and floodwater storage functions of floodplains along Lake Champlain Basin rivers under Vermont's Functioning Floodplain Initiative.

1.0 Introduction

Connected and functioning alluvial floodplains are valued for their ecosystem functions including sediment and nutrient storage, groundwater recharge, and support to aquatic and riparian habitats. Floodplains also have the potential to reduce flood risk to downstream communities by storing floodwaters and attenuating peak discharges. With progressive development, floodplains have become disconnected both laterally and vertically from the river channel, to varying degrees, altering the flux of water and materials (Opperman et al., 2010; Scott et al., 2019). Nearly three-quarters of the Vermont river reaches assessed by VTANR's stream geomorphic assessment (SGA) protocols have lost some degree of floodplain access due to vertical and lateral disconnection (Kline & Cahoon, 2010). In light these historic channel and floodplain changes, floodplain mapping approaches are needed that incorporate this underlying geomorphic data in determining the geographical extents of floodplain inundation.

Floodplains of the Vermont portion of Lake Champlain Basin have been mapped along more than 1700 km of river, and inundation extents and depths for various return intervals have been computed using a probabilistic, low-complexity modeling approach ("probHAND") as part of a separate project (Diehl, et al., 2021a). This modeling approach was built upon hydrologically-defined stream reaches of the National Hydrography Dataset (NHD), and mapping extended up the river networks to reaches draining greater than 10 square miles. Vermont's Functioning Floodplain Initiative (FFI) aims to expand mapping to 2 square miles and transfer this modeling approach from NHD reaches to those of the NHD-compliant, higher-resolution Vermont Hydrography Dataset (VHD), and specifically to define inundation extents for SGA reaches. The goal is to enable spatially-explicit reference to existing channel and floodplain geomorphic data that characterize the degree of vertical and lateral floodplain (dis)connectivity by reach.

To better understand the implications for moving floodplain generation to these finer-resolution reaches, we proposed a pilot study to integrate existing geomorphic assessment data with probabilistic inundation mapping to improve upon estimates and better align floodplain delineations with an existing database of reach-specific stream geomorphic assessment data. We hypothesized that, by incorporating reach breaks that are geomorphically as well as hydrologically defined, a higher-fidelity floodplain extent will be generated from the probHAND modeling approach that will allow for a better interpretation of the influence of reach-scale channel-floodplain configurations on floodplain function and flooding risk. This technical report summarizes key outcomes of this pilot effort carried out in a high-gradient (Mad River) and low-gradient setting (Black Creek).

2.0 Background

In recent years, the widespread availability of remotely-sensed elevation and land cover data has enabled mapping of floodplain inundation using low-complexity hydrologic models at a nationwide to regional scale (Wing et al., 2017; Afshari et al., 2018). The resolution (10 to 30 m pixels) of input data sets to these models is commonly not sufficient to capture channel dimensions and floodplain modifications (e.g., roads, levees, rail berms) that affect estimations of channel storage and incipient floodplain inundation (Afshari et al., 2018) and influence inundation extents (Rebolho et al., 2018). Higher-resolution elevation data (0.7 m resolution) are now available for the whole of Vermont sourced from airborne Light Detection and Ranging (lidar) data (https://vcgi.vermont.gov/data-release/statewide-lidar-coverage-ql2-now-available), and have enabled floodplain mapping at greater resolution (Diehl, et al., 2021b; Gourevitch, et al., 2021). Still, these modeling approaches are subject to limitations in representing the degree of channel-floodplain coupling due to their reliance upon average river geometry calculated over hydrologically-defined reaches that may span sub-reaches of variable valley confinement or slope (Godbout et al., 2019). Additional uncertainty is introduced because the near-infrared laser of the airborne lidar system does not effectively penetrate the water surface to capture channel-bottom elevations (Heidemann, 2018) and thus may under-represent channel bathymetry (Zheng et al., 2018). Hydrodynamic models (e.g., HEC-RAS) that use lidar-derived terrain updated with field-measured channel bathymetry are more accurate than low-complexity models at a site scale, but extension of these methods to model floodplain inundation across the Lake Champlain Basin would be too resource-intensive and computationally intractable, at present. Thus, new low-complexity modeling approaches are needed that incorporate reach-scale geomorphic data for channels and (dis)connectivity status of floodplains to better predict flooding extents and depths, and quantify the uncertainty of these estimates.

3.0 Study Objectives and Tasks

The objective of this study was to evaluate the feasibility of adapting the original probHAND model approach (Diehl et al., 2021a, b) to a larger network (i.e., > 2 mi^2), and using different reach breaks (i.e., SGA), to contribute to the FFI mapping application and framework. We had the additional goal of identifying opportunities to improve upon the efficiency and accuracy of the model, where apparent as we updated the code. Here we report on the results from two contrasting pilot watersheds and identify the challenges and opportunities of mapping floodplains for the full Lake Champlain Basin in Vermont.

Our pilot test included the following specific tasks:

1) Modify the probHAND code and update input files to transfer the analysis from National Hydrography Dataset (NHD) reaches to the higher-resolution, but NHD-compliant Vermont Hydrography Dataset (VHD) to enable spatially-explicit reference to existing channel and floodplain geomorphic data that are georeferenced to the VHD as stream geomorphic

assessment (SGA) reaches. These same SGA reaches are being relied upon in the FFI to characterize the degree of vertical and lateral floodplain (dis)connectivity by reach.

2) Expand the analysis from reaches with a minimum drainage area of 10 mi^2 (26 km^2) to 2 mi^2 (5.2 km^2) to be consistent with mapping extents of Phase 2 of the Functioning Floodplain Initiative; and identify and resolve potential methodological and computational challenges to downscaling.

3) Evaluate the integrity of the downscaled modeling approach by comparing floodplain extents generated from SGA reaches to those generated from a hydraulic model, i.e., 1D HEC-RAS.

4) Compare the floodplain extents generated from NHD reaches to those generated from SGA reaches, and examine potential geomorphic metrics that may account for variability between the two approaches.

3.1 Pilot Study watersheds

We focused our pilot study in two watersheds with contrasting overall gradients (Figure 1):

- Mad River, a moderate- to steep-gradient river draining a 144 mi^2 (373 km^2) subwatershed of the Winooski River basin; and

- Black Creek, a shallow-gradient river draining a 120 mi^2 (311 km^2) subwatershed of the Missisquoi River basin.

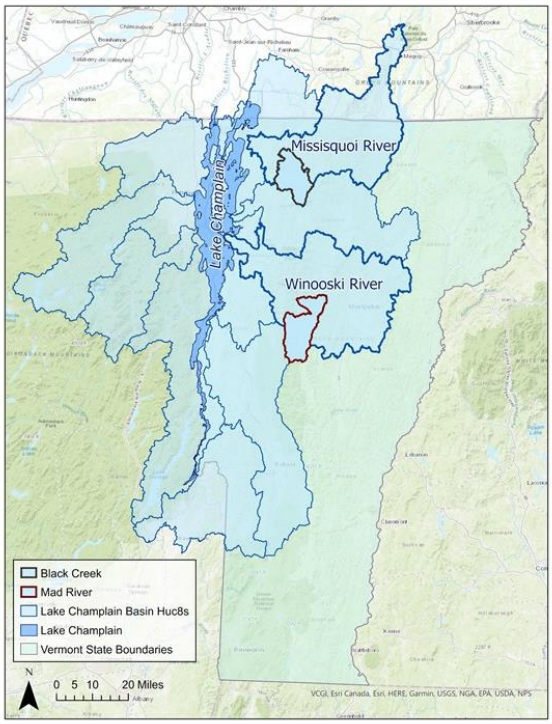

Figure 1. Location of the Mad River and Black Creek pilot project watersheds within the larger study area comprising the Vermont portion of the Lake Champlain Basin.

4.0 Methods

4.1 Overview of probHAND Model

An overview of probHAND is presented below; work flow of the modeling approach is provided in Attachment A; and details of the model are found in Diehl et al. (2021b). The probHAND model references Digital Elevation Models (DEMs) and uses Height Above Nearest Drainage (HAND) mapping tools (Zheng et al., 2018; Nobre et al., 2011) from the Terrain Analysis Using Digital Elevation Models (TauDEM) toolset (Tarboton, 2005) to provide a raster-based estimate of elevation above a specified channel by reach (Figure 2). This *HAND Elevation Raster* is a normalized version of the DEM, wherein each pixel contains a value that equates to the vertical distance from (i.e., elevation difference between) that land-based pixel and the stream-channel pixel to which it drains. For each reach, a synthetic rating curve is calculated that identifies discharge for each stage, or HAND elevation (Figure 2C) (Zheng et al., 2018; Nobre et al., 2011). For a given flood stage, any land-based pixels in the HAND Elevation Raster that have a value less than the stage are considered inundated.

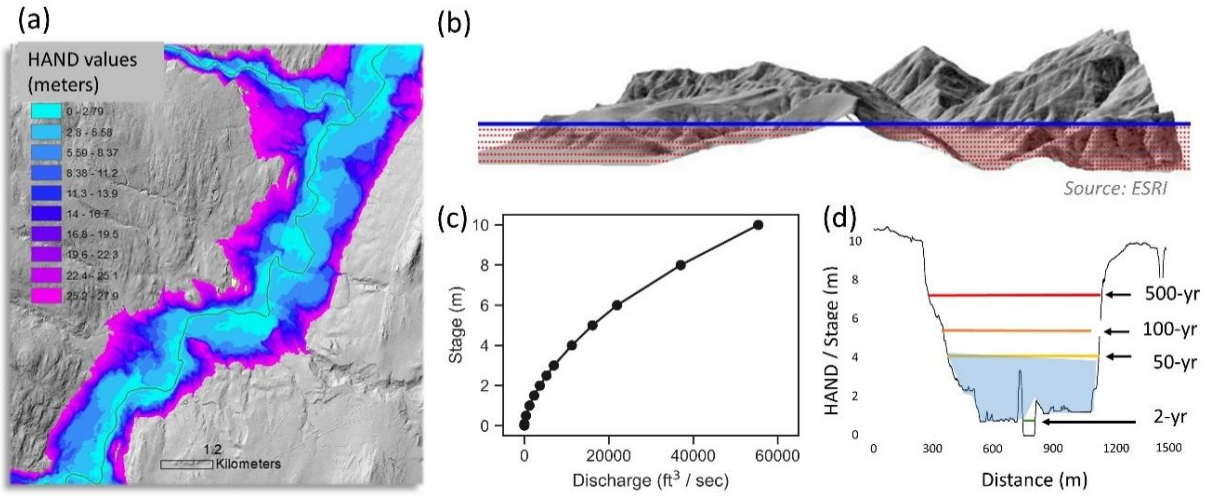

Figure 2. For each reach: (a) the Height Above Nearest Drainage (HAND) is calculated for the active river area. (b) For a series of user-specified horizontal planes (i.e., flood stages), the volume of water above this HAND surface and below each plane is calculated using tools from ESRI's 3D Analyst extension (https://pro.arcgis.com/en/pro-app/tool-reference/3d-analyst/surface-volume.htm). (c) Volume estimates for a series of stages and the Manning's equation are used to construct a stage-discharge relationship; and (d) these stages are related to recurrence interval storms by reference to regional equations (USGS Streamstats; Olson, 2014).

To compute the rating curve within each reach, discharge for a given flood stage, Q, is computed using the Manning's equation, $Q = (1/n)AR_h^{2/3} S^{1/2}$, where cross-sectional area, A, is approximated as the inundation volume in the reach divided by the reach length and hydraulic radius, R_h, is the inundation volume divided by the surface area. These hydraulic geometry data are extracted as average values from the reach-specific channel and floodplain geometry using

Thiessen polygons generated from user-defined reach extents relying on a raster-based stream network. Reach lengths are derived from the attribute data for the stream network and the slope, S, is calculated from the DEM elevations at the start and end of the reach and the reach length. The value for Manning's n is calculated as an area-weighted average of n-values associated with the land-use types present within the inundated area. For this pilot study, we used a 0.5-m resolution land cover/ land use raster sourced between 2013 and 2017 (UVM SAL, 2019) and assigned n-values to land cover classes via a lookup table relying on published values (Acrement & Schneider, 1987, 1989; Chow, 1959; Trueheart, et al., 2020). From the synthetic rating curve, the specific stage that relates to a design-storm discharge (i.e., flood of user-defined Annual Exceedance Probability, AEP) is identified with reference to regional equations (Olson, 2014) using USGS Streamstats and the downstream end of the reach to determine the catchment area (U.S. Geological Survey, 2016).

To account for the uncertainty of this low-complexity hydraulic modeling approach, our probHAND model incorporates a Monte Carlo analysis for input parameters to the Manning's equation (Diehl, et al., 2021b). We assume normal and truncated normal probability distribution functions for Manning's n, slope, cross-sectional area, and discharge. By simulating over 1000 iterations, we generate an empirical cumulative frequency distribution that is mapped to a probabilistic flood inundation surface for each recurrence interval (Figure 3). For a peak flood of given AEP, the probHAND model generates a suite of maps with varying probabilities of inundation based on the ranking of predicted extents from the Monte Carlo simulation, including the 95th, 90th, 75th, 50th, 25th, 10th and 5th percentiles.

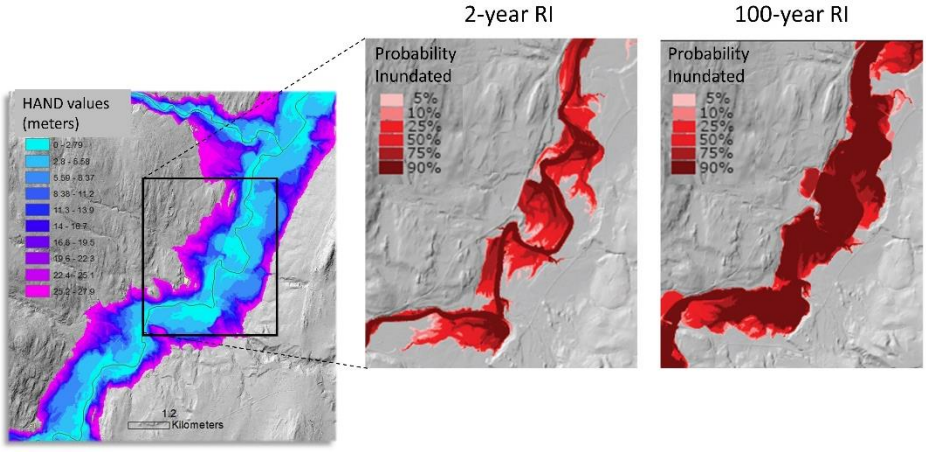

Figure 3. Probabilistic inundation surfaces are generated for floods of various recurrence intervals using a Monte Carlo approach (Diehl et al., 2021b).

4.2 Downscaling of the probHAND approach

Previously, the probHAND analysis for the Lake Champlain Basin (VT portion) was built on reaches defined in the USGS National Hydrological Dataset (NHDPlus), and floodplain mapping was limited to reaches with a drainage area greater than 10 square miles (mi^2). For this pilot test, the probHAND approach was modified to run on Stream Geomorphic Assessment (SGA)

reaches, and simulation coverage was expanded to lower-order streams draining greater than 2 mi^2. In general, SGA reaches are shorter in length than NHDPlus reaches and rather than being only hydrologically defined, (e.g., by tributary confluences), they are also defined geomorphically. SGA reaches are channel lengths of consistent valley-confinement class (i.e., confined, semiconfined or unconfined) within which other channel parameters (e.g., slope, sinuosity, and bedform) are generally consistent (Kline et al., 2009). SGA reach delineations are defined in two phases of stream geomorphic assessment: Phase 1 is largely executed through GIS and remote-sensing steps and defines reaches at a scale of 1: 24,000 from remote-sensing resources including topographic maps and aerial photographs. In Phase 2, reaches may be further divided into segments based on field observations and survey measurements that indicate a substantially different geomorphic character (Kline, et al., 2009). SGA reach and segment breaks were retrieved from the VT Open Geodata Portal and were derived ultimately from the publicly-accessible, VTANR SGA Data Management System [1]. For clarity of presentation, we refer to both SGA reaches and segments as "reaches" in the text below. Modeling was executed in Python and utilized packages: TauDEM 5.3.7, GDAL 2.4.2, geovoronoi 0.1.2, numpy, pandas, geopandas, scipy, os, ogr, osr, sys, gc, datetime, hashlib, ogr, itertools, and argparse.

4.3 Application of probHAND in the Pilot Watersheds

We executed probHAND in the two pilot watersheds using source data and derived data summarized in Attachment B. The first step was to create the *HAND Elevation Raster*, relying on high-resolution (1m), lidar-derived DEMs. that were hydro-enforced using a manual procedure to remove barriers to flow such as culverts and bridges. Hydro-enforced DEMs were then hydrologically conditioned, using a pit-filling procedure, to ensure that pixels along the stream network were non-increasing in elevation with distance in the downstream direction (Zheng et al., 2018). A D-infinity flow accumulation algorithm (Tarboton, 1997) was used to create a landscape-level *Flow Direction Raster* at the HUC12 extent using TauDEM tools. This *Flow Direction Raster* and a *Stream Network Raster* developed at the HUC8 spatial extent were used to determine the elevation relative to the nearest stream network point of each cell along the overland flow paths specified by the *Flow Direction Raster*; these elevations form the *HAND Elevation Raster*. The *Stream Network Raster* was generated at the HUC8 extent because using individual HUC12 DEM rasters to generate stream networks would lead to a discontinuous network where HUC12 boundaries crossed the main stem. To conserve computational resources, the *Stream Network Raster* was developed at a lower-resolution (5 m), which necessitated resampling of the hydro-enforced high-resolution DEMs. Delineating the *Stream Network Raster* required pit-filling and flow direction determination as described above. Using the HUC8-scale *Flow Direction Raster*, a *Flow Accumulation Area* raster was generated. A user-defined flow accumulation threshold was then used to generate the *Stream Network Raster*, which consists of all cells with a drainage area greater than the flow accumulation threshold.

[1] https://anrweb.vt.gov/ DEC/SGA/Default.aspx

To compare the simulated inundation extents under **contrasting stream network densities**, two different *Stream Network Rasters* were used as inputs: streams draining land areas greater than or equal to 10 mi^2 and 2 mi^2 (Figure 4). In practice, the 10 mi^2 limit required a flow accumulation threshold set to 9 mi^2 to generate full coverage of channel reaches at the upstream termini of the river network. A 1.5 mi^2 flow accumulation threshold was tested for the 2 mi^2 stream network, but was found to introduce stream network artifacts; therefore, a threshold of 2 mi^2 was used for the 2 mi^2 stream network. Reaches that were only partially mapped (due to drainage areas less than the threshold) were excluded from comparisons. A quantitative analysis was carried out to compare inundation extents built on these stream networks of contrasting density in the Mad River watershed only, because of the availability of a HEC-RAS model and a FEMA floodplain for most of the model domain that would serve as a reference data set for comparison of probHAND-simulated inundation extents under the two stream network densities.

To compare the simulated inundation extents under **contrasting reach-break definitions**, two options for reach delineation were analyzed in each watershed: 1) NHDPlus reaches (at 1:100,000 resolution) and 2) SGA reaches defined at 1:24,000 resolution during field-based stream geomorphic assessments (Figure 5). This analysis used the 10 mi^2 *Stream Network Raster* files in both pilot watersheds, Mad River and Black Creek. In the Mad River, this included a 24.4-mile length of the main stem and a 2.3-mile length of the Mill Brook tributary. In the Black Creek, analysis took place on a 23.7-mile length of the main stem and a 3.3-mile length of the Fairfield River tributary. A quantitative analysis (see Section 4.4) was carried out to compare inundation extents built on these stream networks of contrasting reach-break definition.

4.4 Evaluating probHAND model integrity

To evaluate the integrity of the modeled floodplain extents, we quantified differences in inundated areas between modeling approaches, following methods of Afshari and others (2018). A fitness-statistic (F-stat) was calculated with a resulting value in the range from 0 (no agreement) to 1 (full agreement) to consider the number of conforming wet cells predicted by both models. The F statistic was calculated as follows:

$$F = \frac{C_{m1+m2}}{C_{m1} + C_{m2} - C_{m1+m2}},$$

where C_{m1+m2} is the number of cells predicted wet by both models, C_{m1} is the number of wet cells predicted by Model 1 when the same cells in the Model 2 domain may or may not be wet, and C_{m2} is the number of wet cells predicted by Model 2 when the same cells in the Model 1 domain may either be wet or dry. An overall F-statistic was calculated as a linear-weighted average relying on the reach lengths. Model comparisons (Table 1) used the 1% AEP flood extent, because this is the design storm most often relied upon for FEMA Flood Insurance Rate Mapping and assessment of community risk. Specifically, we used the 50th percentile 1% AEP map, because in previous testing the 50th percentile probHAND map exhibited the closest agreement to a map generated from a 1D HEC-RAS model for the equivalent design storm (Diehl et al., 2021b).

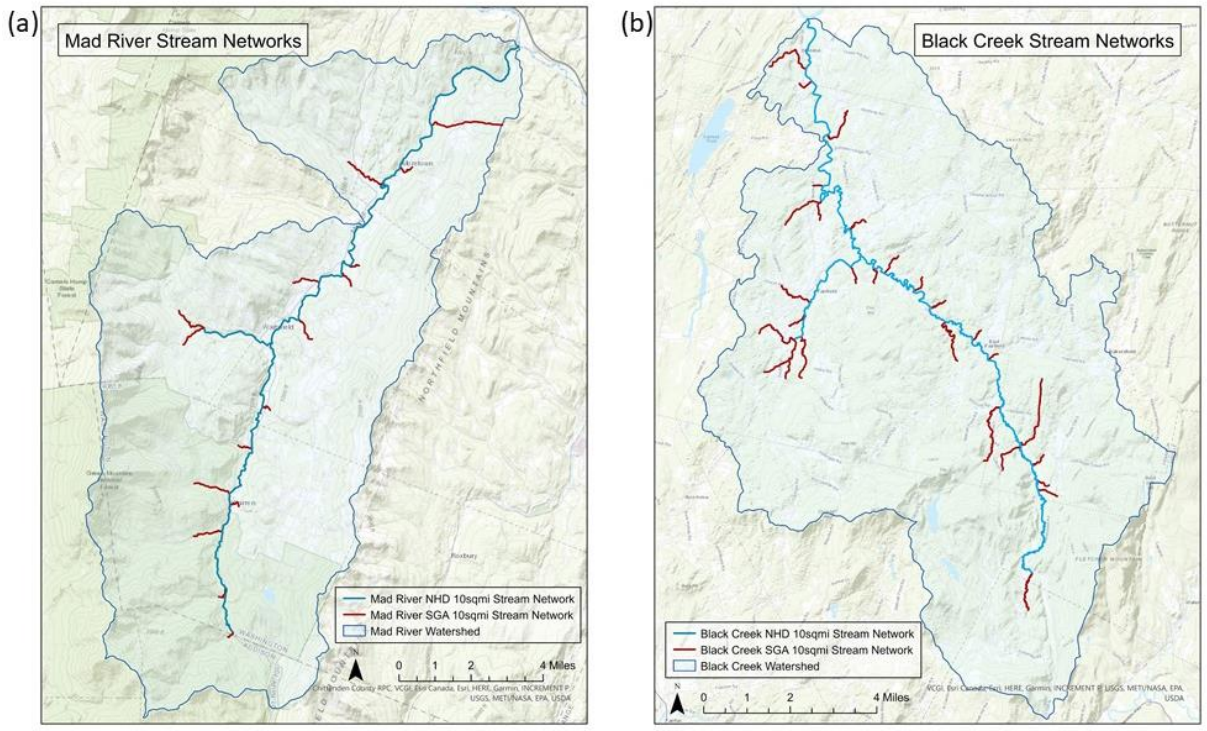

Figure 4. Modeling extents in the pilot watersheds, (a) Mad River and (b) Black Creek, showing NHD reaches (in blue) overlain on SGA reaches (in red).

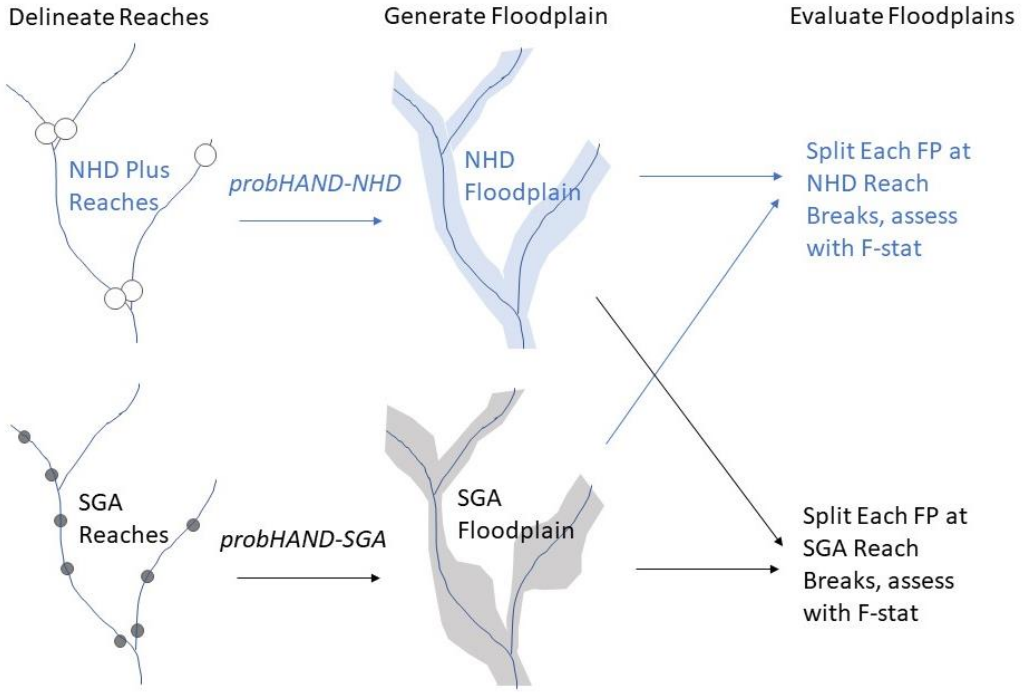

Figure 5. Illustration of work flow to evaluate integrity of floodplains mapped using contrasting definition of reach breaks - NHD vs SGA (Analysis #3 in Table 1).

In the Mad River, we compared our prob-HAND generated SGA and NHD floodplain extents to two reference floodplains available for the same 1% AEP design storm: (1) a 1D HEC-RAS model simulation built on lidar DEMs sourced in 2013 and augmented with channel cross sections collected in 2016 (Dubois & King, 2017); and (2) a more dated FEMA floodplain that is the current zoning reference for communities in the watershed, built on cross section data sourced in the late 1970s and 1980s (FEMA, 2013).

Table 1. Model comparisons for specific floodplain analyses.

Analysis	Model 1	Model 2
1. Contrasting stream network densities – Mad River	Q100 floodplain built on SGA or NHD reaches	Q100 floodplain generated from 1D HECRAS model
2. Contrasting stream network densities – Mad River	Q100 floodplain built on SGA or NHD reaches	Q100 floodplain generated by FEMA
3. Contrasting reach-break definition – Mad River and Black Ck	Q100 floodplain built on NHD reaches	Q100 floodplain built on SGA reaches

4.5 Evaluate Influence of Geomorphic Metrics

We evaluated if geomorphic metrics (e.g., valley confinement, channel slope, incision ratio, entrenchment ratio, stream order, drainage area, etc) were correlated to fitness-statistic values for SGA- and NHD-defined floodplains, using consistent SGA-reach breaks. Reach length, slope and reach inundation area were sourced from the probHAND workflow, with reference to the DEMs. Upstream drainage area for each SGA reach was calculated using USGS Streamstats (https://streamstats.usgs.gov/ss/). Valley confinement ratios, incision ratios and entrenchment ratios were exported from the VTANR SGA Data Management System (https://anrweb.vt.gov/DEC/SGA/Default.aspx) – which archives results of field-based geomorphic assessments (Kline et al., 2009). Because not all reaches had been fully assessed in the field, these latter ratios were only available for a subset of the study reaches (n=40).

5.0 Results and Discussion

The existing probHAND approach was modified in several ways to accommodate analysis at the scale of SGA reaches, as well as an expansion of mapping extents to the drainage density with minimum drainage area of 2 mi^2. Modifications successfully enabled generation of floodplain extents at this finer-scale, and geomorphically-relevant, reach resolution and greater mapping extent under the FFI. Geomorphic-based SGA reaches improved agreement in hydraulically complex areas of our two pilot watersheds, such as in town centers and in wide valleys with low gradients. Yet we identified important limitations in source data that will influence the transfer of these approaches at the scale of the Lake Champlain Basin (or state-wide).

5.1 Changes to original probHAND inputs and approach

To pilot the expansion of floodplain maps to a larger stream network, and to evaluate the changes in model performance with a change in reach breaks, we identified improvements to the original probHAND workflow, code, and pre- and post-processing steps (as described in Diehl et al., 2021b). Modifications are summarized in Attachment C.

The biggest change in work flow was implemented to address the observation that lidar-derived DEMs were not sufficiently hydro-enforced; this condition was more prevalent on tributaries and became more of a concern as we expanded mapping coverage to 2 square miles. Unaddressed barriers to flow (e.g., bridge decks, culverts) caused flow routing algorithms to generate large errors in the *HAND Elevation Raster* and, consequently, in the synthetic rating curves and inundation maps. To resolve this issue, we manually edited the DEMs to remove hydrologic barriers. In one HUC12 of the Black Creek (MSQ_0501), where we first identified this issue, the hydro-enforced DEM significantly altered inundation extents in places (Figure 6). The inundation map using the hydro-enforced DEM, and NHD-defined reaches, identified a much narrower floodplain than with the original DEM (F = 0.70).

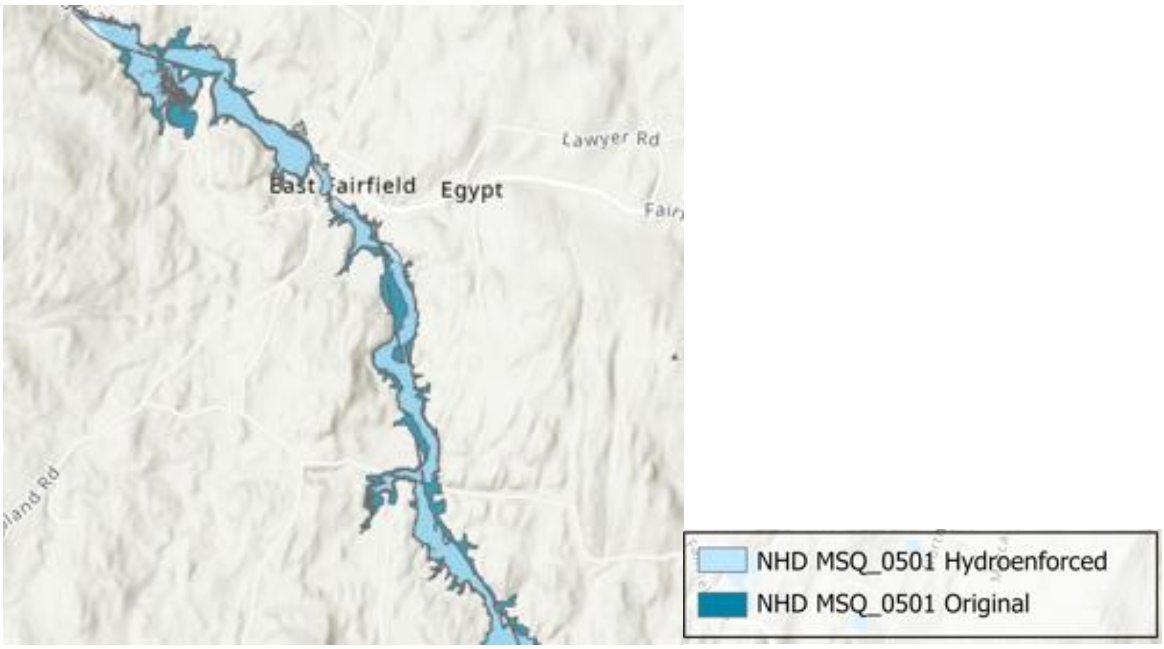

Figure 6. Example of differences in inundation of 100-year floodplain (50th percentile) on the Black Creek (MSQ_0501) using a fully hydro-enforced DEM compared to one that was not fully hydro-enforced, i.e., "Original".

The second key area of work flow modification centered around pre-processing steps required to facilitate probHAND analysis at the scale of SGA reaches. NHDPlus data sets include a unique numerical code by reach that stores information about flow direction and accumulation in the stream network. This reach code is relied upon within probHAND work flow to extract stage-specific hydraulic geometry information for each reach, and to calculate area-weighted

Manning's roughness values from the underlying land cover/land use data. A similar unique code exists for SGA reaches (i.e., the "SGAT ID" number), but it is composed of combinations of numerals, letters, and punctuations that are somewhat inconsistently applied across the state-wide geomorphic data set. Because the alpha-numeric SGAT IDs of SGA reaches would be problematic for operations within the existing code, a new numbering scheme was developed and implemented for SGA reaches within our pilot watersheds.

Once the above workflow modifications were implemented (largely through manual methods), we were able to successfully generate floodplains built on SGA reaches for comparison to floodplains built on NHD reaches for further evaluation.

5.2 Comparison of floodplain extents for probHAND vs. HEC-RAS and FEMA

For the overall main stem of the Mad River, probHAND floodplains built on SGA and NHD reaches had a similar performance when compared to the 1D HEC-RAS floodplain for the 1% AEP event (Table 2). When further examined at a reach scale, the SGA floodplain better represented steeper, naturally confined reaches (Figure 7). In our Mad River study area, these reach types coincided with village centers of Moretown, Waitsfield and Irasville which were historically established near bedrock reaches to exploit the water power for mill operations (Beers, 1873) – a pattern common throughout the Northeastern U.S. (Johnson et al., 2019).

In general, the SGA floodplain mapped to the extent of 2 mi^2 drainage areas had a similar performance as the floodplain developed on the 10 mi^2 extent when compared to the HEC-RAS floodplain. Both the SGA and NHD floodplains showed lesser agreement with the FEMA floodplain than with the HEC-RAS floodplain; this result may be due in part to the outdated nature of this FEMA layer. Our study made reference to the 1% AEP FEMA floodplain available in digital form effective 2013; however, this digital update relied on floodplain/channel cross sections obtained in the late 1970s and early 1980s (FEMA, 2013). Since these earlier cross sections were measured, several large floods have occurred in the Mad River watershed (including events in 1998 and 2011 with recurrence intervals of 21 and 85 years, respectively) resulting in substantial modification of the channel planform and dimensions (Jordan, 2013).

Table 2. Comparison of probHAND-modeled floodplains to HEC-RAS and FEMA floodplains for the 100-year design storm.

Comparison	F-statistic
SGA floodplain (9 mi^2) to HEC-RAS Floodplain	0.81
NHD floodplain (9 mi^2) to HEC-RAS Floodplain	0.80
SGA floodplain (2 mi^2) to HEC-RAS Floodplain	0.80
SGA floodplain (9 mi^2) to FEMA Floodplain	0.71
NHD floodplain (9 mi^2) to FEMA Floodplain	0.71

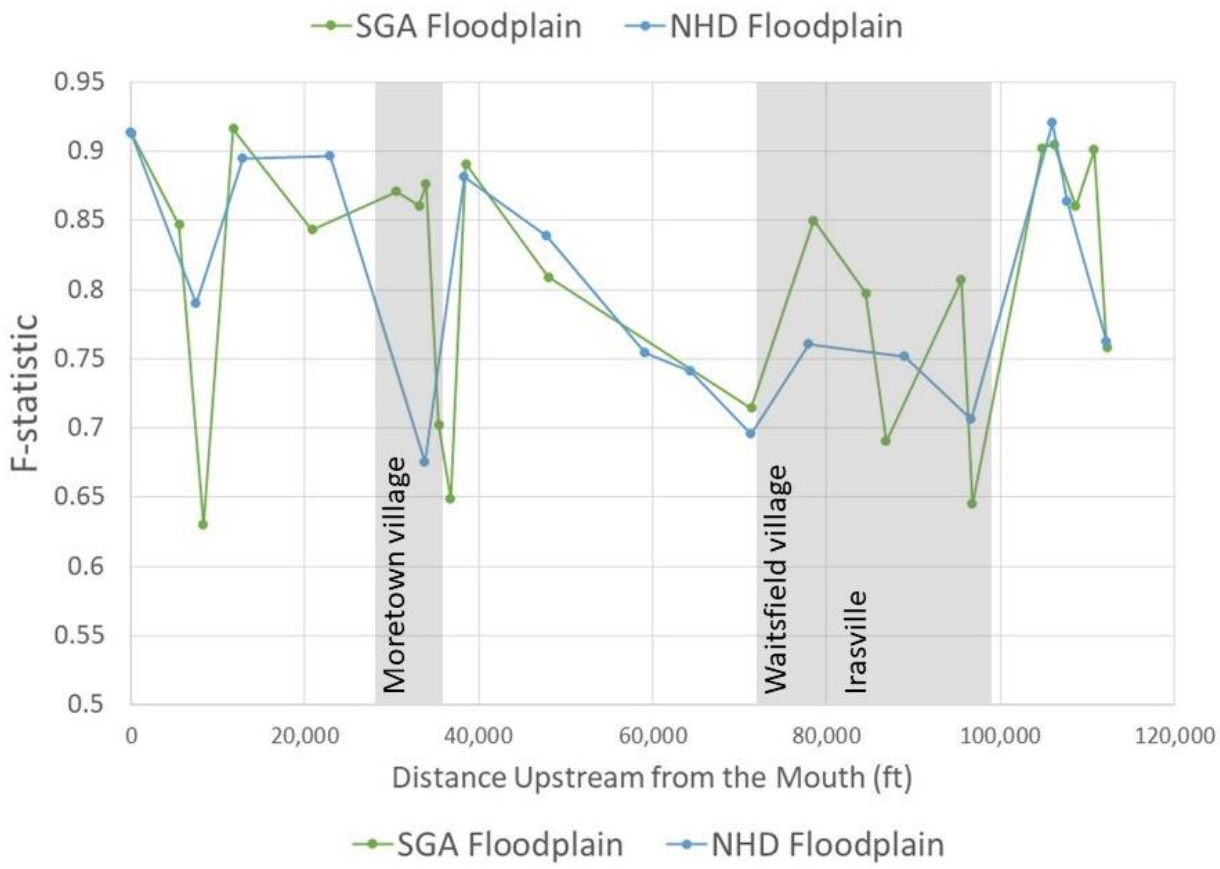

Figure 7. Longitudinal profile of reach-scale performance of probHAND-modeled floodplains built on SGA vs NHD reaches in the Mad River relative to the HEC-RAS floodplain. Gray shading indicates regions where SGA performance exceeded NHD performance (coinciding with village centers). Nodes indicate the downstream end of SGA or NHD reaches.

5.3 Comparison of probHAND simulations built on SGA vs NHD reaches

Stream networks based on contrasting reach definition (SGA vs NHD) generated somewhat different inundation extents (Figure 8). The SGA reaches were generally shorter in length than NHD reaches, although not exclusively (Table 3). The lower-gradient and lower-relief Black Creek study area had a greater percentage of mapped floodplains (2.5 mi^2, or 2.1%) than the Mad River study area (1.9 mi^2, 1.4%).

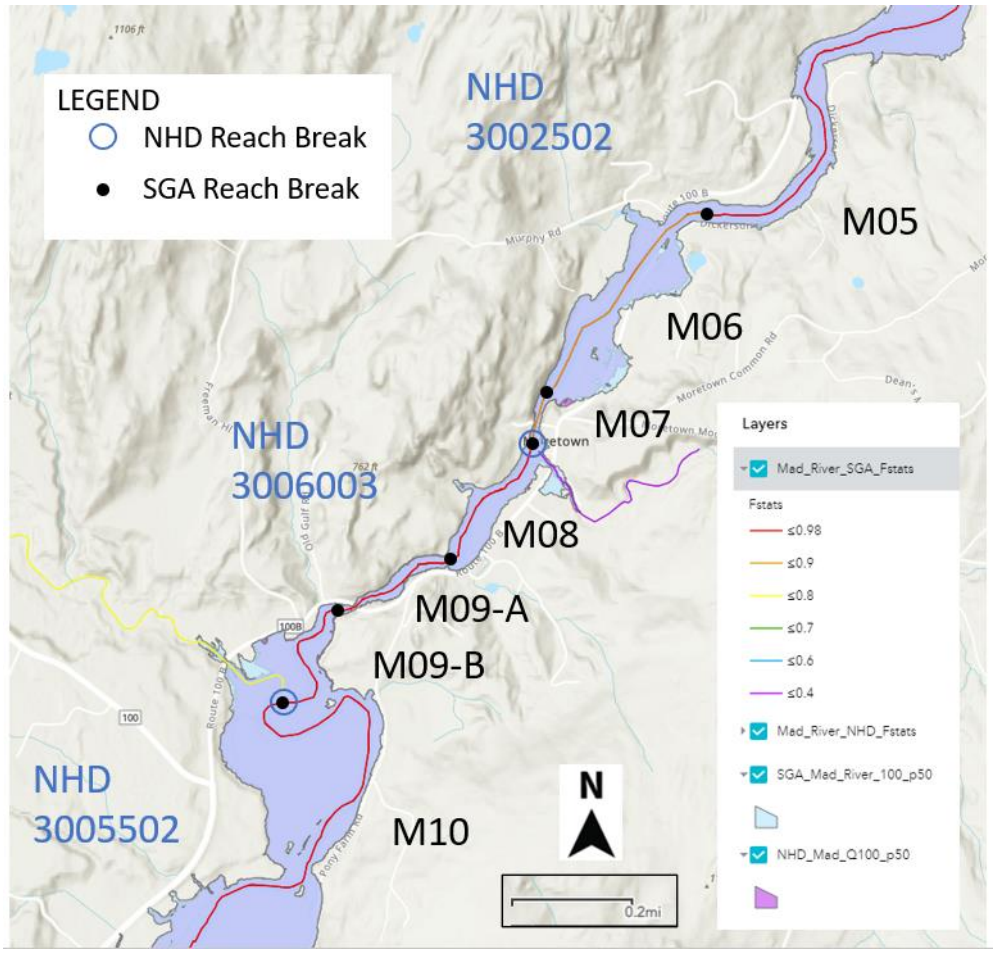

Figure 8. Example of NHD vs. SGA reach extents in portion of the Mad River main stem in vicinity of Moretown, VT.

Table 3. Summary of study reaches for pilot testing in the Mad River and Black Creek.

Parameter	Units	Min	Max	Median	Mean	Total
NHD Plus Reaches (n = 38)						
Length	feet	292	29,765	5,431	7,456	283,322
Reach Inund Area	acres	1.1	427	39	79	3,017
F stats	--	0.37	0.98	0.90	0.86	--
F stats LW	--				0.88	
SGA Reaches (n = 49)						
Length	feet	439	23,362	3,695	5,801	284,226
Reach Inund Area	acres	2.0	422	27	58	2,830
F stats	--	0.46	1.00	0.95	0.92	--
F stats LW	--				0.93	

Overall, floodplains generated using SGA reach breaks had greater linear-weighted F-statistic scores than floodplains built using NHD reach breaks. The shift to SGA reach breaks, from NHD reach breaks improved the agreement in inundation extents between the two approaches to reach segmentation by 5.6%. The improvement was more apparent in the low-relief Black Creek (8% improvement) than in the higher-relief Mad River watershed (4.5%; Figure 9).

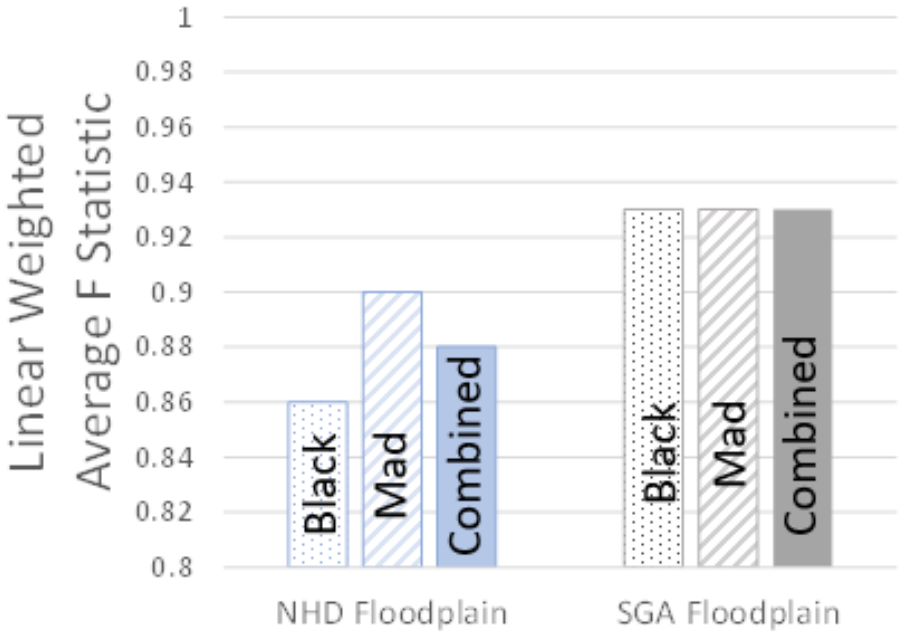

Figure 9. Average linear-weighted F-statistic scores for NHD vs. SGA floodplains calculated for Black Creek reaches, Mad River reaches, and the two watersheds combined.

Three study area reaches had lower-than-average F statistics, and represent outliers in this analysis. NHD and SGA floodplains were in poor agreement (F= 0.46) in reach M05-A of the Black Creek just upstream from the tributary confluence of Fairfield River (Figure 10). A similar confluence effect from smaller tributaries may have contributed to a low F-stat (F = 0.64) in reach T4.05-B of that Fairfield River tributary (not pictured).

The probHAND approach relies on the Manning's Equation and underlying assumptions of steady-state uniform flow to compute discharge in each reach. This discharge is then related to stage (inundation depth) through a synthetic rating curve constructed from reach-average geometry. Because there is no continuity between reaches (i.e., discharge is not routed through the stream network); this condition leads to discontinuities between reaches which may be especially pronounced at tributary confluences.

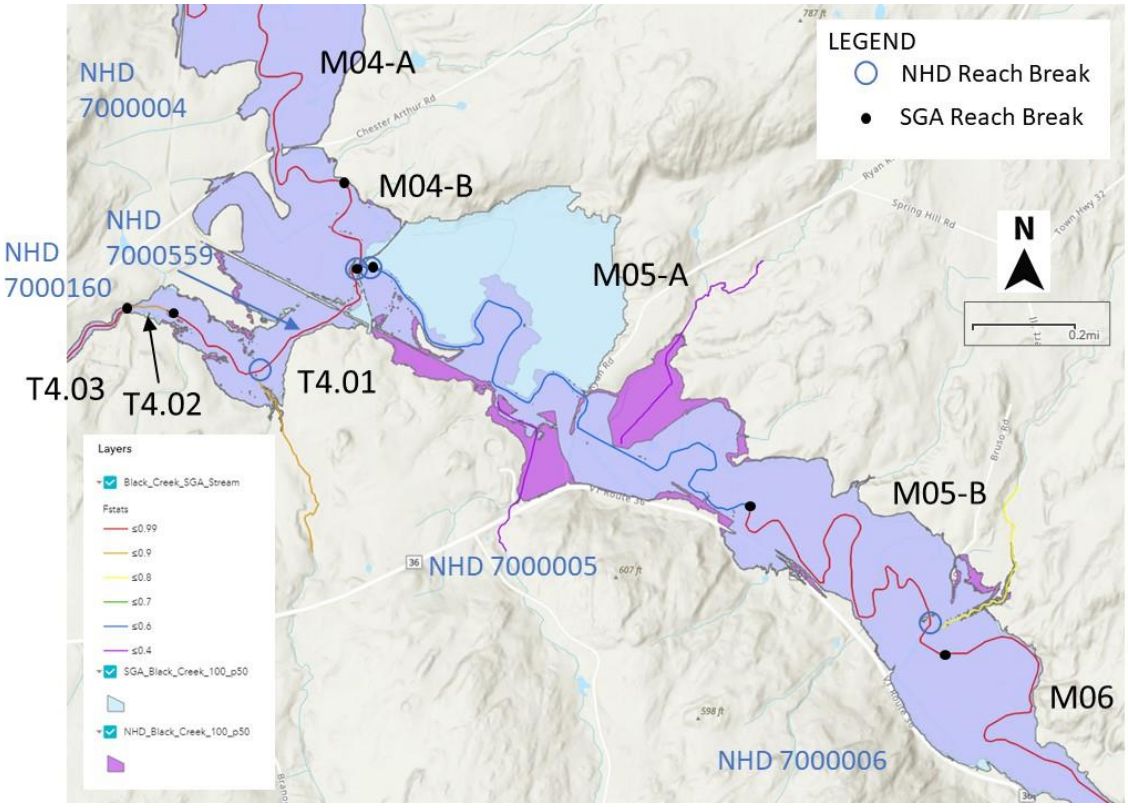

Figure 10. NHD and SGA floodplains were in poor agreement along the Black Creek main stem (SGA reach M05-A) just upstream from the Fairfield River tributary (tributary T4).

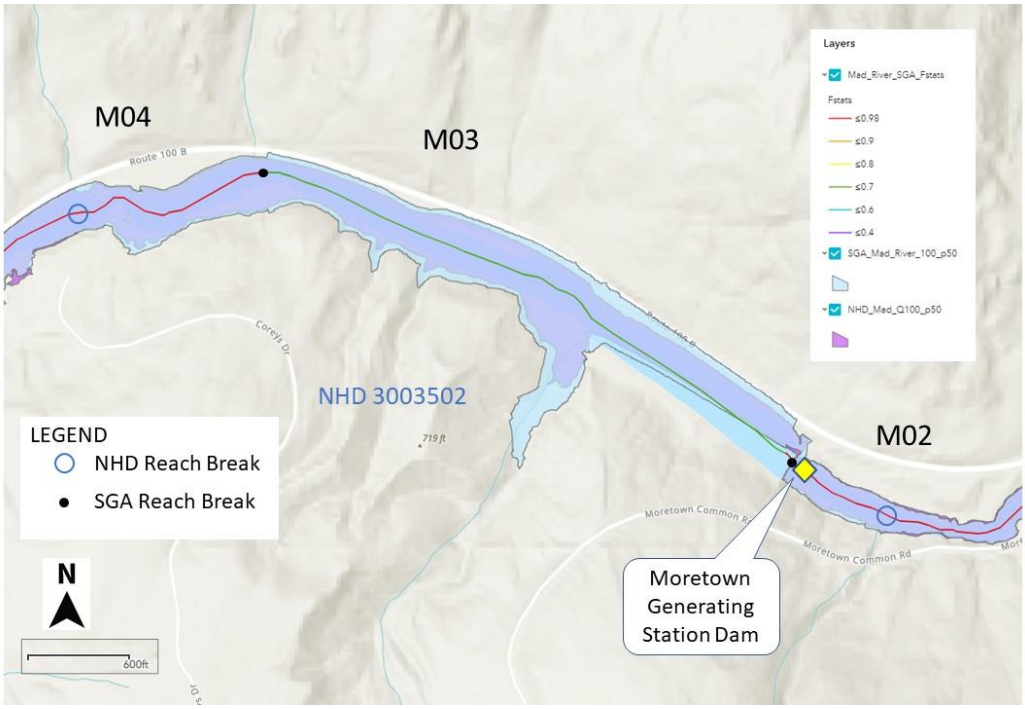

Figure 11. Differing placement of reach breaks for NHD vs SGA in vicinity of a hydroelectric dam may have contributed to localized, poor agreement between NHD and SGA floodplains.

Poor agreement (F= 0.69) between NHD and SGA floodplains in a third study reach on the Mad River was influenced by presence of a hydroelectric dam and its location relative to contrasting reach end points under the NHD versus SGA delineations (Figure 11). This dam has a vertical drop of approximately 36 feet (Dubois & King, 2017). The SGA reach ends just upstream of this vertical drop (M03; 0.03%). In contrast, the NHD reach delineated in this vicinity spans this vertical drop, and therefore has a steeper channel slope (NHD 3003502; 0.73%). The shallower reach-average gradient and higher average channel bed elevation of the M03 reach delineation led to a higher predicted inundation stage (and greater inundation area) for the SGA floodplain upstream of the dam, as compared to the NHD floodplain.

5.4 Analysis of geomorphic metrics as explanatory variables for F-stats values

For the forty SGA reaches with field-measured stream geomorphic data, the NHD and SGA floodplains showed greater agreement where those reaches were closely confined by valley walls (Figure 12), consistent with findings of others (Zheng et al., 2018). Confined reaches are naturally entrenched (i.e., have low entrenchment ratios) due to close coupling of the valley walls (i.e., valley width less than 4 times the channel width), and consequently their inundation areas are less sensitive to shifts in stage.

Overall, there was greater uncertainty in floodplain extents (i.e, more disagreement between NHD and SGA floodplain extents) in unconfined settings than in confined settings. Unconfined reaches, where valley width was more than 4 times the channel width, would naturally have greater entrenchment ratios, but may become entrenched by virtue of floodplain encroachments (e.g., roads, rails) that have reduced the available floodprone width (Blanton and Marcus, 2009) and/or as a result of channel incision in response to natural and human disturbances (Simon and Rinaldi, 2006; Underwood et al., 2021). Unconfined reaches in the study area, thus, exhibited a wide range of entrenchment values (Figure 12). Within the unconfined reaches, the agreement between NHD and SGA floodplains generally increased as the entrenchment ratio increased (Figure 12) – i.e., as the floodprone width became much larger than the bankfull width. In these settings (e.g., Rosgen E, C, D channels), the channel volume is a smaller fraction of the overall channel-floodplain conveyance, and the error introduced by under-representation of channel bathymetry may become less influential.

In unconfined channels with relatively low entrenchment ratios, the bankfull channel cross section represents a larger proportion of the floodprone width cross section, and under-representation of the maximum channel depth (from reliance on infrared-lidar-derived DEMs) may inordinately influence the stage of the bankfull discharge and higher design storm discharges.

Perhaps because of this limited vertical resolution of lidar-derived DEMs in direct vicinity of the river channel, incision ratios available from field assessments were not strongly correlated to F-statistic values in unconfined reaches in our study areas. Neither were reach slope, length, or drainage area strongly correlated to F-statistic values in our pilot watersheds.

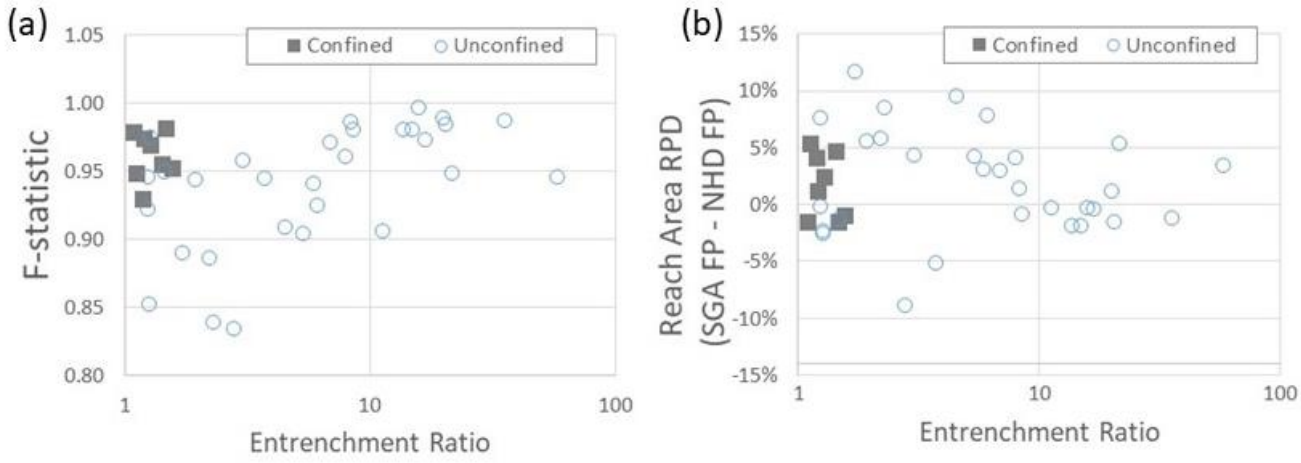

Figure 12. Valley confinement was a governing factor in the variability between SGA and NHD floodplains, with (a) confined reaches of low entrenchment ratio exhibiting larger F-statistic values than unconfined reaches; and (b) smaller Relative Percent Difference values than unconfined reaches (n = 38; 2 outlier reaches removed). Negative RPD values indicate that reach inundation area for the NHD floodplain was greater than that for the SGA floodplain; positive RPD values indicate that the reach-based SGA floodplain was greater in area than the NHD floodplain.

5.5 Implications for transfer of the downscaling approach to Lake Champlain Basin

Despite the successful downscaling of the probHAND modeling approach to SGA reaches in our two pilot watersheds, we identified that the insufficiency of input data sets at two key steps in the overall workflow present important limitations for transfer of this downscaling approach to the scale of the greater Lake Champlain Basin under current timelines of Phase 2 of the Functioning Floodplain Initiative.

To enable more accurate inundation mapping, the DEMs that underlie the probHAND modeling work flow need to be hydrologically enforced, or hydro-enforced, to remove barriers to flow such as culverts. While the metadata for DEMs may describe them as a hydro-enforced product (Heidemann, 2018), in reality, many crossing structures exist that have not been removed and lead to pit-filling errors. Through efforts of our research team, additional funding has been secured from the Vermont Center for Geographic Information in FY2022 that is supporting the Spatial Analysis Lab to conduct improved hydro-enforcing of DEMs for the Lake Champlain Basin.

Secondly, preprocessing of the VHD stream network to reflect uniquely-numbered SGA reaches defined by Phase 1 and Phase 2 Stream Geomorphic Assessments, requires considerable manual effort. We have prototyped an automated method of reach code assignment and reach tree generation, but operationally this approach is limited by the discontinuous nature of the current version of the VHD stream network that contains gaps at tributary confluences. Additionally,

existing GIS layers of SGA reaches do not always represent the most updated information available through the Rivers Program, and the current SGA Phase 1 and Phase 2 stream reach data sets contain data gaps and data-sparse regions (e.g., Otter Creek and Lamoille River basins; Figure C1). To address these challenges, we have an opportunity to leverage Vermont's high-resolution DEMs using established geospatial analysis tools (e.g., FACET, GUT), to infill geomorphic reach delineations in data-sparse regions of the LCB (and state). This remote-sensing based product ("SGA Light") fused with the existing geomorphic data set (https://anrweb.vt.gov/DEC/SGA/Default.aspx) would ensure a more consistent SGA-defined stream network, and could be annotated with the necessary attributes to support the probHAND model work flow.

6.0 Conclusions

Using an existing probabilistic low-complexity hydraulic modeling approach (probHAND), floodplain inundation modeling in two pilot watersheds has been successfully adapted to downscale analysis to the generally finer resolution of reaches defined during stream geomorphic assessments. Mapping has also been expanded to reaches draining 2 mi^2 or larger. Geomorphic as well as hydrologic definition of reaches has enabled spatially-explicit reference to data that characterize the degree of vertical and lateral floodplain (dis)connectivity by reach being compiled for Vermont rivers under the Functioning Floodplain Initiative.

Floodplain mapping built on SGA rather than NHD reach extents captured greater variability in inundation patterns in reaches where the topography was more complex, notably in proximity to town centers, in the vicinity of vertical discontinuities such as bedrock falls or dams. Greater uncertainty in floodplain extents (i.e., more disagreement between NHD and SGA floodplains) was observed in unconfined reaches than in settings of close valley confinement. Incised reaches and reaches with close Holocene stream terraces (Dunn et al., 2007), exhibited low entrenchment ratios and were associated with greater uncertainty of floodplain inundation extents.

Within the unconfined reaches, the agreement between SGA and NHD floodplains generally increased as the valley width increased in relationship to bankfull width, and the channel volume represented a smaller fraction of the overall channel-floodplain conveyance. Low-complexity hydraulic modeling would be improved in all settings by availability of DEMs derived from airborne bathymetric lidar surveys (e.g., green lidar) able to penetrate water and better represent channel volumes.

With additional investments to improve input data sets, the state of Vermont could realize improved accuracy of floodplain inundation extents using this low-complexity hydraulic mapping approach that incorporates geomorphic reach breaks rather than hydrologically-defined NHD reaches. These methods would have wide application in other mountainous regions of the US and would be expected to improve fidelity of inundation maps in steeper terrain composed of mixed alluvial and bedrock channel types. Geomorphic reach delineations could be developed

for these areas using remote-sensing approaches relying on high-resolution lidar, which is becoming increasingly available in other parts of the country.

While this work has identified approaches to improve fidelity of mapped inundation extents on floodplains, there is an additional need to estimate the frequency, duration and timing of these flooding events to better understand the risks to humans and built infrastructure, and the potential benefits of inundation for sediment and nutrient storage, flood peak attenuation, and support to aquatic and riparian habitats. Future improvements to the probHAND modeling approach are being explored, including integrating flow duration curves and cluster analysis to identify flooding duration classifications for Lake Champlain Basin subwatersheds.

7.0 Acknowledgements

This material is based upon work supported by the U.S. Geological Survey under Grant/Cooperative Agreement No. (G16AP00087) to the Vermont Water Resources and Lake Studies Center. KU, RD, and SD were each supported in part by funding from the VT Department of Environmental Conservation and Watershed Investment Division under Phase 2 of the Functioning Floodplain Initiative. KU, RD, and SD also received funding from the Vermont Water Resources and Lake Studies Center (and ultimately USGS). Funding from the Lake Champlain Basin Program partly supported RD and KU. PhD Candidate, JM, was supported by a GUND Barrett Fellowship. The project team is grateful to Jesse Gourevitch for technical advice on HAND methodology and software; JG was partially supported by the GUND Institute for Environment and VT EPSCoR.

8.0 References

Acrement Jr., G.J., Schneider, V.R., 1987. Roughness Coefficients for Densely Vegetated Flood Plains: USGS Water-Resources Investigations Report 83-4247, 71p., available at https://pubs.er.usgs.gov/publication/wri834247.

Acrement Jr., G.J., Schneider, V.R., 1989. Guide for Selecting Manning's Roughness Coefficients for Natural Channels and Flood Plains: USGS Water Supply Paper 2339, 38p., available at https://pubs.er.usgs.gov/publication/wsp2339.

Afshari, S., A. A. Tavakoly, M. A. Rajib, X. Zheng, M. L. Follum, E. Omranian, and B. M. Fekete. (2018). Comparison of new generation low-complexity flood inundation mapping tools with a hydrodynamic model. *Journal of Hydrology* 556:539-556.

Beers, F.W., Ed. (1873). Atlas of Washington County, Vermont. New York, NY: F.W. Beers & Co.

Blanton, P., W. A. Marcus. 2009. Railroads, roads, and lateral disconnection in the river landscapes of the continental United States. Geomorphology 112:212-227.

Chow, V.T., 1959. *Open Channel Hydraulics*, Blackburn Press, Caldwell, NJ.

Diehl, R.M., Wemple, B.C., Underwood, K.L., Ross, D. (2021a). "Evaluating floodplain potential for sediment and phosphorus deposition: Development of a framework to assist in Lake Champlain Basin planning" Report to the Lake Champlain Basin Program, draft submitted January 20, 2021.

Diehl, R.M., Gourevitch, J.D., Drago, S., Wemple, B.C. (2021b). Improving flood risk datasets using a low-complexity, probabilistic floodplain mapping approach. *PLoS ONE*, 16 (3), e0248683, https://doi.org/10.1371/journal.pone.0248683

Dubois & King, Inc. (2017). Flood Study: Mad River Area, prepared for Central Vermont Regional Planning Commission, available at: http://centralvtplanning.org/wp-content/uploads/2019/02/Flood-Study-of-the-Mad-River-Area-Report-DK-5.31.17.pdf

Dunn, R., Springston, G., and Donahue, N. (2007). Surficial Geologic Map of the Mad River Watershed, Vermont, Vermont Geological Survey Open File report, VG07-1.

Federal Emergency Management Agency. (2013). Flood Insurance Study, Washington County, VT. Study Number 50023CV001A.

Godbout, L., Zheng, J.Y., Dey, S., Eyelade, D., Maidment, D. and Passalacqua, P., 2019. Error assessment for height above the nearest drainage inundation mapping. *JAWRA Journal of the American Water Resources Association*, *55*(4), pp.952-963.

Gourevitch, J.D. Diehl, R.M., Wemple, B.C., and Ricketts, T. 2021. Inequities in the distribution of flood risk under floodplain restoration and climate change scenarios. *People and Nature*, accepted

Heidemann, Hans Karl, 2018, Lidar base specification (ver. 1.3, February 2018): U.S. Geological Survey Techniques and Methods, book 11, chap. B4, 101 p., https://doi.org/10.3133/tm11b4.

Johnson, K.M., Snyder, N.P., Castle, S., Hopkins, A.J., Waltner, M., Merritts, D.J., Walter, R.C. (2019). Legacy sediment storage in New England river valleys: Anthropogenic processes in a postglacial landscape. *Geomorphology*, *327*, 417–437.

Jordan, L. (2013). Stream Channel Migration of the Mad River between 1995 and 2011. University of Vermont, Honors College Thesis. Available at: https://www.uvm.edu/sites/default/files/S13_Thesis_Jordan.pdf

Kline, M., & Cahoon, B. (2010). Protecting River Corridors in Vermont. *Journal of the American Water Resources Association*, 1(10). doi: 10.1111/j.1752-1688.2010.00417.x

Kline, M., C. Alexander, S. Pytlik, S. Jaquith, and S. Pomeroy (2009). Vermont Stream Geomorphic Assessment Protocol Handbooks. Vermont Agency of Natural Resources, Waterbury, Vermont. http://dec.vermont.gov/watershed/rivers/river-corridor-and-floodplain-protection/geomorphic-assessment.

Nobre, A.D., Cuartas, L.A., Hodnett, M., Renno, C.D., Rodrigues, G., Silveira, A., Waterloo, M., Saleska, S. (2011). Height above the Nearest Drainage - a hydrologically relevant new terrain model. *J. Hydrol.*, 404: 13-29, doi: 10.1016/j.jhydrol.2011.03.051

Olson, S. A. (2014). Estimation of flood discharges at selected annual exceedance probabilities for unregulated, rural streams in Vermont, *with a section on* Vermont regional skew regression, by Veilleux, A. G., *Scientific Investigations Report 2014–5078*, U.S. Geological Survey, Washington, D. C., doi:10.3133/sir20145078.

Opperman, J. J., Luster, R., McKenney, B.A., Roberts, M., Meadows, A.W. (2010). Ecologically Functional Floodplains: Connectivity, Flow Regime, and Scale. *Journal of the American Water Resources Association, 46*(2):211-226. https://doi.org/10.1111/j.1752-1688.2010.00426.x.

Rebolho, C., Andréassian, V. and Moine, N.L., 2018. Inundation mapping based on reach-scale effective geometry. *Hydrology and Earth System Sciences*, *22*(11), pp.5967-5985.

Scott, D.T., Gomez-Velez, J.D., Jones, C.N., Harvey, J.W. (2019). Floodplain inundation spectrum across the United States. *Nat. Commun*., 10, 5194, doi:10.1038/s41467-019-13184-4

Simon A., Rinaldi, M. (2006). Disturbance, stream incision, and channel evolution: the roles of excess transport capacity and boundary materials in controlling channel response. *Geomorphology* 79, 361–83.

Tarboton, D. G. (1997). A New Method for the Determination of Flow Directions and Contributing Areas in Grid Digital Elevation Models. *Water Resources Research* 33(2): 309-319

Tarboton, D. G. (2005). Terrain Analysis Using Digital Elevation Models Version 5, Utah Sate University, Logan [Software], available at: https://hydrology.usu.edu/taudem/taudem5/downloads.html (last access: 20 May 2021).

Trueheart, M.E., Dewoolkar, M.M., Rizzo, D.M., Huston, D., Bomblies, A. (2020). Simulating hydraulic interdependence between bridges along a river corridor under transient flood conditions. Science of the Total Environment 699: 134046, https://doi.org/10.1016/j.scitotenv.2019.134046.

Underwood, K. L., Rizzo, D.M., Dewoolkar, M.M., and Kline, M. (2021). Analysis of Reach-scale Sediment Process Domains in Glacially-conditioned Catchments Using Self-Organizing Maps. *Geomorphology*, doi: 10.1016/j.geomorph.2021.107684

University of Vermont Spatial Analysis Laboratory. (2019). Vermont High Resolution Land Cover [dataset], available at: https://geodata.vermont.gov/pages/land-cover.

U.S. Geological Survey, 2016, The StreamStats program, online at http://streamstats.usgs.gov, last accessed on 20 August 2021.

Wing, O. E. J., Bates, P.D., Sampson, C.C., Smith, A.M., Johnson, K.A., Erickson, T.A. (2017). Validation of a 30m resolution flood hazard model of the conterminous United States. *Water Resour. Res.* **53**, 7968–7986, doi:10.1002/2017WR020917.

Zheng, X., D.G. Tarboton, D.R. Maidment, Y.Y. Liu, and P. Passalacqua. 2018. River Channel Geometry and Rating Curve Estimation Using Height above the Nearest Drainage. *J. Amer. Wat. Res. Assoc*., 54 (4): 785-806. doi:10.1111/1752-1688.12661.

Attachment A. Overview of probHAND modeling approach

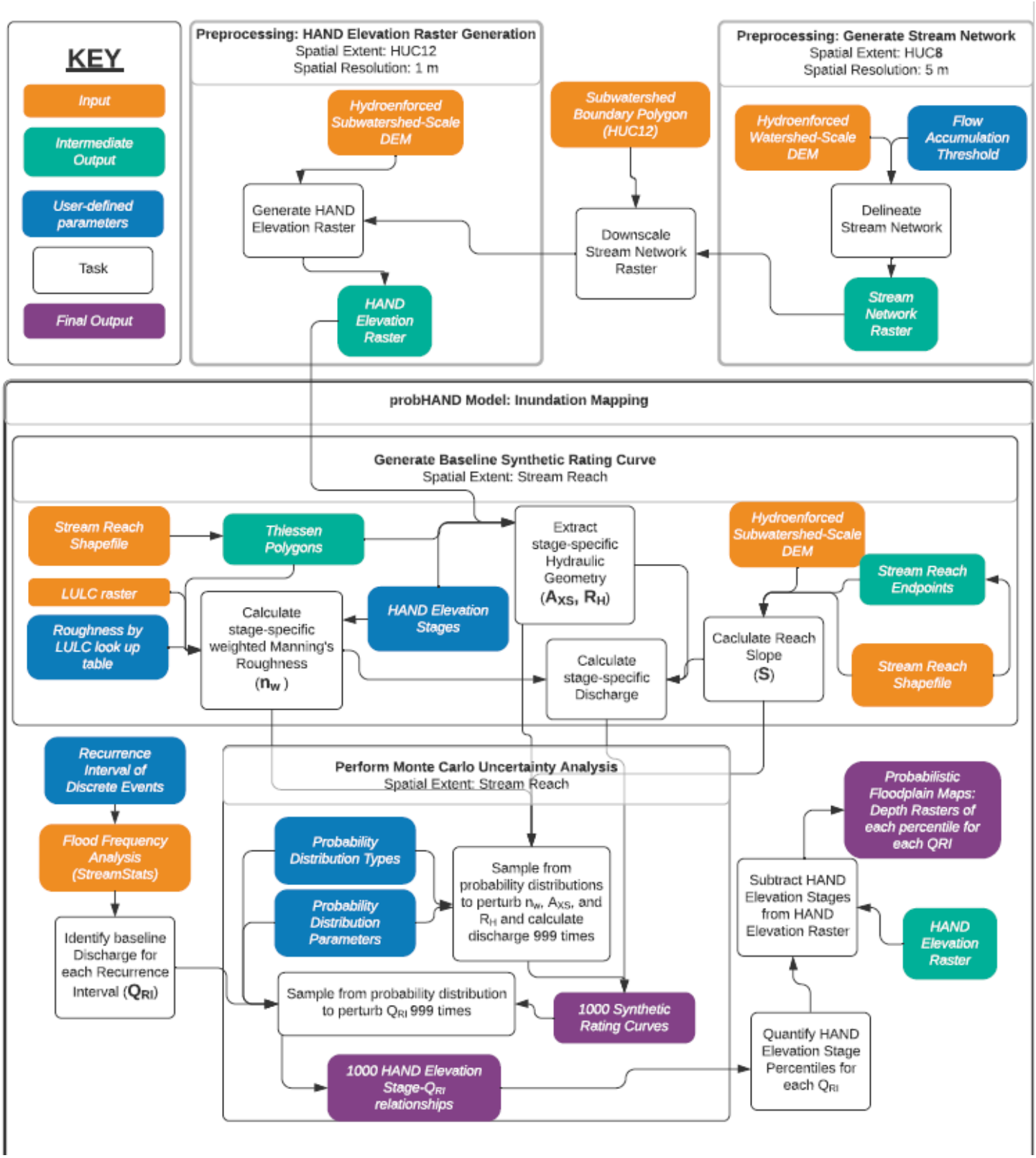
KEY
Input
Intermediate Output
User-defined parameters
Task
Final Output
Preprocessing: HAND Elevation Raster Generation
Spatial Extent: HUC12
Spatial Resolution: 1 m
Hydroenforced Subwatershed-Scale DEM
Generate HAND Elevation Raster
HAND Elevation Raster
Subwatershed Boundary Polygon (HUC12)
Downscale Stream Network Raster
Preprocessing: Generate Stream Network
Spatial Extent: HUC8
Spatial Resolution: 5 m
Hydroenforced Watershed-Scale DEM
Flow Accumulation Threshold
Delineate Stream Network
Stream Network Raster
probHAND Model: Inundation Mapping
Generate Baseline Synthetic Rating Curve
Spatial Extent: Stream Reach
Stream Reach Shapefile
Thiessen Polygons
LULC raster
Roughness by LULC look up table
Calculate stage-specific weighted Manning's Roughness (n_w)
HAND Elevation Stages
Extract stage-specific Hydraulic Geometry (A_{XS}, R_H)
Hydroenforced Subwatershed-Scale DEM
Stream Reach Endpoints
Caclulate Reach Slope (S)
Stream Reach Shapefile
Calculate stage-specific Discharge
Recurrence Interval of Discrete Events
Flood Frequency Analysis (StreamStats)
Identify baseline Discharge for each Recurrence Interval (Q_{RI})
Perform Monte Carlo Uncertainty Analysis
Spatial Extent: Stream Reach
Probability Distribution Types
Probability Distribution Parameters
Sample from probability distributions to perturb n_w, A_{XS}, and R_H and calculate discharge 999 times
Sample from probability distribution to perturb Q_{RI} 999 times
1000 Synthetic Rating Curves
1000 HAND Elevation Stage-Q_{RI} relationships
Probabilistic Floodplain Maps: Depth Rasters of each percentile for each QRI
Subtract HAND Elevation Stages from HAND Elevation Raster
HAND Elevation Raster
Quantify HAND Elevation Stage Percentiles for each Q_{RI}

Attachment B. Data sets: source, intermediate and outputs

Table B-1. **Original data sets** utilized in the probHAND model for pilot testing in the Mad River and Black Creek.

Data	Type	Analysis Extent	Description	Application	Resolution	Source Date(s)	Reference
HUC12 watershed boundaries	Polygon	HUC12	Outlines of the HUC12 watershed areas (both with and without buffers)	Used to clip rasters to HUC12 extents	1:24,000	2014	https://geodata.vermont.gov/datasets/VCGI::vt-subwatershed-boundaries-huc12/about
Digital Elevation Model (DEM)	Raster	HUC12	Lidar-derived, hydro-flattened Digital Elevation Model, hydroenforced, tiled mosaic, clipped to buffered HUC12	Used to generate landscape-level *HAND Elevation Raster* and cell-by-cell drainage directions using D∞ algorithm	1 m	2013 (Mad River), 2017 (Black Creek)	https://maps.vcgi.vermont.gov/LidarFinder/
Stream Reach Shape file	Polyline	≥ 10 mi^2	NHDPlus split at NHD reaches	Used to generate Theissen polygons that facilitate extraction of reach-averaged hydraulic geometry values. Reach breaks also used to delineate upstream drainage areas and query USGS Streamstats for peak discharge values at a suite of design storms.	1:100,000	2017	https://geodata.vermont.gov/documents/VCGI::national-hydrography-dataset/about
	Polyline	≥ 2 mi^2	VHD split at reaches/segments defined by VTANR Stream Geomorphic Assessment protocols		1:24,000	2001 - 2016	https://geodata.vermont.gov/documents/VCGI::vt-hydrography-dataset-high-resolution-nhd/about https://geodata.vermont.gov/datasets/VTANR::sga-phase-2-assessed-reaches/about https://geodata.vermont.gov/datasets/VTANR::sga-phase-2-reach-segment-breaks/about https://geodata.vermont.gov/datasets/VTANR::sga-reach-breaks/about
Land Cover/ Land Use	Raster	HUC12	Vermont High Resolution Land Cover	Used to define a reach-average weighted Manning's roughness coefficient specific to each stage (i.e., inundation extent) for use in the Manning's equation.	0.5 m	2013-2017 LiDAR data and 2016 NAIP imagery	https://geodata.vermont.gov/pages/land-cover

Table B-2. **Intermediate Outputs** developed during execution of probHAND.

Data	Type	Analysis Extent	Description	Application	Reso-lution	Source Files
Lower-resolution DEM	Raster	HUC8	1-m resolution hydroenforced DEMs (HUC12 scale) tiled to cover the HUC8 extent and re-sampled to a 5-m resolution.	Used to generate the *Lower-resolution pit-filled DEM*	5 m	Hydroenforced DEMs covering the HUC8 extent (1m, HUC12)
Lower-resolution pit-filled DEM	Raster	HUC8	The *Lower-resolution DEM* with any sinks (areas that are surrounded by cells at a higher elevation) filled to the pour-over elevation	Used to generate the *Lower-resolution flow direction raster*	5 m	Lower-resolution hydroenforced DEM (5m, HUC8)
Lower-resolution flow direction raster	Raster	HUC8	The proportion of the flow volume that will flow to each of two down-slope cells based on the D∞ angle of flow	Used to generate the *Lower-resolution flow accumulation area raster*	5 m	Lower-resolution pit-filled DEM (5m, HUC8)
Lower-resolution flow accumulation raster	Raster	HUC8	The area draining into each cell based on the direction raster	Used to generate the *Lower Resolution Stream Network Raster*	5m	Lower-resolution flow direction raster (5m, HUC8)
Lower-resolution Stream Network Raster	Raster	HUC8	A raster where any cell with a contributing drainage area greater than a user-defined threshold has a value of 1 and all other cells have a value of 0	Used to generate the *Stream Network Raster* for each HUC12	5 m	Lower-resolution flow accumulation raster (5m, HUC8); User-defined flow accumulation threshold

Stream Network Raster	Raster	HUC12 (un-buffered)	The *Lower-resolution Stream Network Raster* clipped to the HUC12 extent and resampled to 1m resolution	Used to generate the *Hand Elevation Raster*	1 m	Lower-resolution Stream Network Raster (5m, HUC8); HUC12 watershed boundary shapefile (un-buffered)
Buffered Pit-filled DEM Raster	Raster	HUC12 (buffered)	The buffered hydroenforced DEM with sinks filled to the pour-over elevation	Used to generate the *Buffered Flow Direction Raster* and the *Pit-filled DEM Raster*	1 m	Buffered Hydroenforced DEM (1m, HUC12)
Pit-filled DEM Raster	Raster	HUC12 (un-buffered)	The buffered hydroenforced DEM with sinks filled to the pour-over elevation	Used to generate the *HAND Elevation Raster*	1 m	Buffered pit-filled DEM (1m, HUC12)
Buffered Flow Direction Raster	Raster	HUC12 (buffered)	The proportion of the flow volume that will flow to each of two down-slope cells based on the D∞ angle of flow	Used to generate the *Flow Direction Raster*	1 m	Buffered pit-filled DEM (1m, HUC12)
Flow Direction Raster	Raster	HUC12 (un-buffered)	The *Buffered Flow Direction Raster* with garbage edge data clipped out	Used to generate the *HAND Elevation Raster*	1m	Buffered Flow Direction Raster (1m, HUC12); HUC12 watershed boundary shapefile (un-buffered)
HAND Elevation Raster	Raster	HUC12 (un-buffered)	The elevation of each cell above the nearest drainage cell along an overland flow path	Used to extract reach-averaged parameters for use in Manning's Equation and to estimate depth and extent of inundation for a given design storm flow rate	1m	Flow Direction Raster (1m, HUC12); Pit-filled DEM Raster (1m, HUC12)
Stream Points (NHD or VHD)	Point shapefile	HUC12 (un-buffered)	The stream polylines converted to points	Used to extract min and max elevations for each reach and to		Stream reach shapefile (either NHD or VHD)

				generate *Thiessen polygons*		
Thiessen polygons (NHD or VHD)	Raster	HUC12 (un-buffered)	A raster where each cell is assigned to the nearest reach (as measured by Euclidean distance)	Used to extract reach-averaged parameters from the *HAND Elevation Raster*	1m	Stream Points (based on either the NHD or the VHD stream reach polylines)

Table B-3. **Model outputs** generated during execution of probHAND.

Data	Type	Analysis Extent	Description
Synthetic Rating Curve Logbook	Table	Reach	A table of reach parameters (length, surface area, volume, cross-sectional area, hydraulic radius, Manning's n, and slope) and Manning's discharge for a variety of stages for each of the 1000 iterations of the Monte Carlo analysis
Storm-Inundation Logbook	Table	Reach	A table of estimated inundation stages (as interpolated from the synthetic rating curves) for the 2, 5, 10, 25, 50, 100, 200, and 500 year design storm flows for each of the 1000 iterations of the Monte Carlo analysis.
Probabilistic Inundation Extents	Raster	HUC12 (un-buffered)	Inundation extents for each reach and for each design storm based on the 5^{th}, 10^{th}, 25^{th}, 50^{th}, 75^{th}, 90^{th}, and 95^{th} percentiles of the depths calculated during the Monte Carlo analysis.

Attachment C. Details of probHAND modifications

Details of ProbHAND modifications

Application of probHAND in the Lake Champlain Basin, and downscaling to the finer-resolution stream network defined by VTANR SGA segments and reaches, has necessitated several modifications to the overall probHAND modeling approach (Diehl et al., 2021b), including pre-processing and post-processing steps. Modifications are summarized below, and organized by the key interim and final steps of the simulation.

C.1 Pre-processing steps

C.1.1 HAND Elevation Raster

<u>DEM quality</u>

DEMs required hydrologic conditioning, using a pit-filling procedure, to ensure that pixels along the stream network are non-decreasing in elevation with distance in the downstream direction (Zheng et al., 2018). This conditioning procedure is contained within the TauDEM tool. The pit-filling procedure can create artifacts when the underlying DEMs are not sufficiently hydro-enforced.

We developed a Python tool that subtracts the pit-filled raster from the original DEM – to create a raster of filled pits for visual inspection. This tool revealed that many of the Lake Champlain Basin (LCB) DEMs are not sufficiently hydro-enforced. While the metadata for DEMs describes them as a hydro-enforced product, in reality, many crossing structures exist that have not been hydro-enforced and lead to pit-filling errors.

We developed a standard method/approach for hydro-enforcing DEMs – being implemented by the UVM Spatial Analysis Lab (SAL) under direction of our UVM FFI team. Through efforts of our research team, funding has been secured from the Vermont Center for Geographic Information in FY2022 that is supporting the Spatial Analysis Lab to conduct improved hydro-enforcing of DEMs for the Lake Champlain Basin (158 HUC12s).

C.1.2 Stream Network Raster

To conserve computational resources, the code was modified to generate the *Stream Network Raster* from a lower-resolution (5m) DEM. This necessitated resampling of the hydro-enforced high-resolution DEMs, and a subsequent pit-filling step at this coarser resolution.

The flow accumulation threshold used to define the *Stream Network Raster* has changed from a hard-wired threshold to a user-defined threshold. Note that the *Stream Network Raster* produced in probHAND preprocessing steps will differ somewhat from the stream network that is cartographically mapped in NHDPlus or VHD.

C.2 probHAND Model: Inundation Mapping

C.2.1 Baseline Synthetic Rating Curve

Stream Reach Shapefile

NHDPlus data sets include a unique numerical code by reach that stores information about flow direction and accumulation in the stream network. This reach code is relied upon within probHAND work flow to extract stage-specific hydraulic geometry information for each reach, and to calculate area-weighted Manning's roughness values from the underlying land cover/land use data. A similar unique code exists for SGA reaches (i.e., the SGAT ID number), but it is composed of combinations of numerals, letters, and punctuation that are somewhat inconsistent in their application across the state-wide geomorphic data set. Therefore, to run probHAND model simulations at the finer-scale of SGA reaches, a new numbering scheme was developed for SGA reaches, since the alpha-numeric SGAT IDs of SGA reaches would be problematic for operations within the existing code.

Considerable manual effort is required to assign a unique numeric code to each reach. We attempted to develop an automated method of code assignment, but operationally this was limited by the discontinuous nature of the VHD stream network that has been split at reach breaks and segment breaks.

We developed a reach tree to indicate the upstream and downstream reaches adjacent to a subject reach in the stream network. This reach tree was developed primarily to enable a quality-assurance check of the reach-specific data compiled from USGS Streamstats. It would also have application in a future dynamic version of probHAND to approximate flood wave routing through the stream network.

Additional factors would limit transfer of downscaling methods outside of the pilot watersheds to the spatial extent of Lake Champlain Basin or the state of Vermont. GIS layers of SGA reaches do not always represent the most updated information available through the Rivers Program, and the current SGA Phase 1 and Phase 2 stream reach data sets contain data gaps and data-sparse regions (e.g., Otter Creek basin, Lamoille River basin, Figure C1). To address these challenges, we have an opportunity to leverage Vermont's high-resolution DEMs using established geospatial analysis tools (e.g., FACET, GUT), to infill geomorphic reach delineations in data-sparse regions of the LCB (and state). This remote-sensing based product ("SGA Light") fused with the existing stream geomorphic data set (https://anrweb.vt.gov/DEC/SGA/Default.aspx) would ensure a more consistent SGA-defined stream network, and could be annotated with the necessary attributes to support the probHAND model work flow.

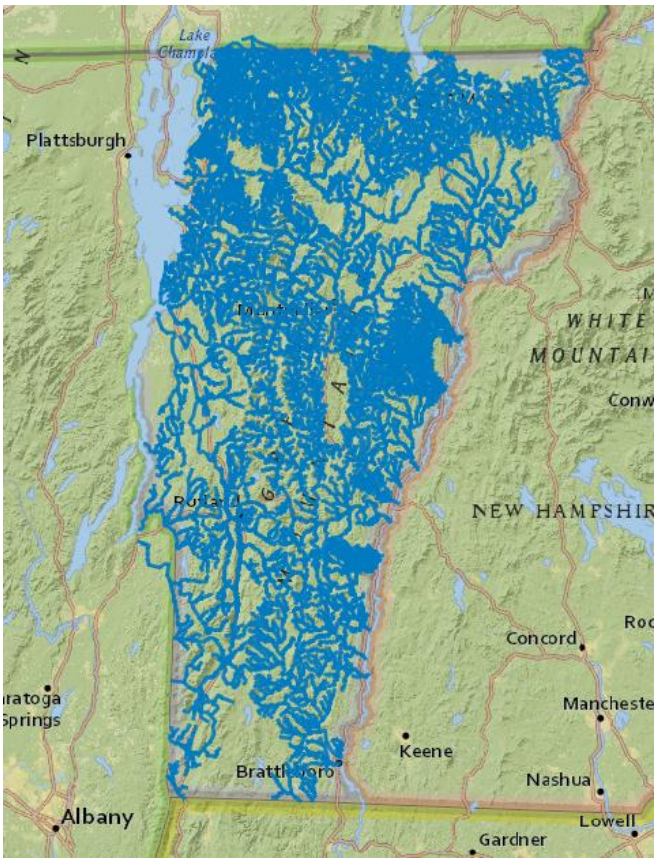

Figure C1. Stream network in Vermont that has been delineated into geomorphic reaches and segments. Downloaded from VT Open Geo Data Portal, August 2021.

Stream Reach Endpoints

We shifted from a previous approach that established reach points at the center of the NHD reach to an approach that defines reach points at the downstream end of the reach (either NHD or SGA). This change was made to be more consistent with data development under stream assessment protocols (VTANR, 2009) and the FFI. Reach endpoints are referenced to calculate reach slope from underlying DEMs, and to estimate reach-average hydraulic geometry to compute discharge for each simulated stage.

The code was also modified to address a data gap in the VTANR SGA Data Management System – i.e., calculating channel slope derived for segments. If a reach was segmented into one or more pieces during Phase 2 Stream Geomorphic Assessments, those segments may (often) have channel slopes that differ considerably from the slope of the overall reach (stored in the Phase 1 data set). Yet, there is no field in the Phase 2 data set to store a calculated channel slope for the segments. We modified the probHAND code to store this slope information derived from the DEM, since it is a necessary step in the development of data for Manning's equation by reach and segment. These data could also support the VTANR Rivers Program and users of the FFI.

Reach endpoints are also used in batch requests to USGS Streamstats (U.S. Geological Survey, 2016) to determine upstream catchment area and compute design-storm discharge (i.e., flood

of user-defined Annual Exceedance Probability, AEP). These design storm discharges that rely on regional equations (Olson, 2014) are then referenced to determine a corresponding stage using the synthetic rating curve for each reach.

C.2.2 Monte Carlo Uncertainty Analysis

No substantial modifications to this section of the code have been made at this time.

C.3 Post-Processing

Visualization and Display of probHAND products

Relying on simulations from the Monte Carlo analysis of probHAND, we have prototyped methods to incorporate probability information in displays of inundation extents (Figure C2). These probability layers are being used in the FFI to develop more spatially-explicit forecasts of sediment and phosphorus deposition on floodplains.

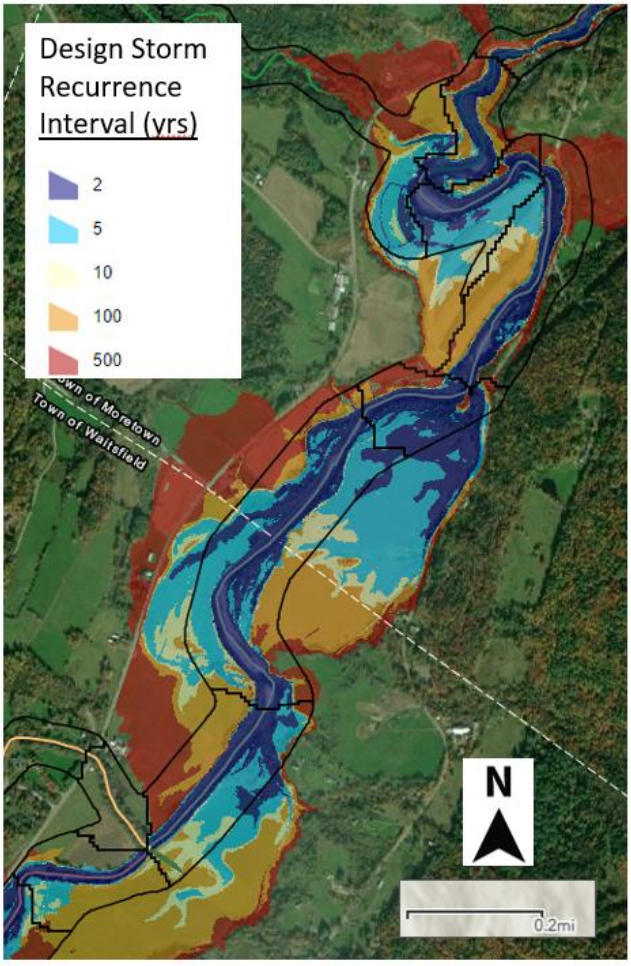

Figure C2. Probabilistic mapping of floodplain extents modeled from probHAND.